

ON THE REVERSIBILITY OF ADVERSARIAL ATTACKS

Chau Yi Li*, Ricardo Sánchez-Matilla, Ali Shahin Shamsabadi, Riccardo Mazzon, Andrea Cavallaro

Centre for Intelligent Sensing, Queen Mary University of London, UK

ABSTRACT

Adversarial attacks modify images with perturbations that change the prediction of classifiers. These modified images, known as adversarial examples, expose the vulnerabilities of deep neural network classifiers. In this paper, we investigate the predictability of the mapping between the classes predicted for original images and for their corresponding adversarial examples. This predictability relates to the possibility of retrieving the original predictions and hence reversing the induced misclassification. We refer to this property as the reversibility of an adversarial attack, and quantify reversibility as the accuracy in retrieving the original class or the true class of an adversarial example. We present an approach that reverses the effect of an adversarial attack on a classifier using a prior set of classification results. We analyse the reversibility of state-of-the-art adversarial attacks on benchmark classifiers and discuss the factors that affect the reversibility.

Index Terms— Adversarial perturbations, Adversarial example, Deep neural network, Reversibility

1. INTRODUCTION

Deep Neural Networks (DNNs) for visual classification tasks achieve high average accuracy in predicting the true class labels in benchmark datasets [1, 2]. However, DNNs are vulnerable to perturbations that modify an original image to mislead the classifier [3, 4]. These modified images, known as adversarial examples, facilitate the study of the robustness of DNN classifiers [5]. Adversarial examples have also been used to conceal private information in images by precluding a classifier from identifying specific class labels [6].

Studies of adversarial examples analysed the relationship between the classes predicted for the adversarial examples (*adversarial classes*) and the corresponding *true classes* of the original images [7], and between the adversarial classes and the classes predicted for the original images (*original classes*) [6]. However, the possibility of retrieving the original predictions from the adversarial class, a property which we refer to as *reversibility*, has so far been neglected.

In this paper, we argue that reversibility is a fundamental property of an adversarial attack, and propose to quantify the extent to which an attack may be reversed. We achieve this goal by analysing the mapping between the predicted classes of original images and those of adversarial examples generated by an attack. We discuss the reversibility of state-of-the-art attacks on benchmark classifiers and investigate the factors affecting the reversibility. Moreover, we

present an approach to perform Prediction Reversal from the Adversarial Class (PRAC) using the prediction results of a set of original images and their corresponding adversarial classes. Specifically, for each adversarial class, we obtain the probabilities that its original images would be predicted to be of a particular original class. Our previous work on reversibility analysed the dissimilarity between the frequency distribution of adversarial classes and a uniform distribution, without attempting to retrieve the original class [6].

PRAC is useful for designers of adversarial attacks and defences. In fact, PRAC allows an attack designer to quantify the extent to which the attack can be reversed, whereas a defence designer may label a set of adversarial examples and use PRAC to retrieve the original and true class of new adversarial examples generated with the same attack.

2. CLASS MAPPING

Let $C(\cdot)$ be a D -class DNN classifier that predicts the class of an image to be one in $\{y_1, \dots, y_i, \dots, y_D\}$. Let the output of an original image x passing through all but the last layer of the classifier, $L(\cdot)$, be defined as

$$L(x) = (p(y_1|x), p(y_2|x), \dots, p(y_D|x)), \quad (1)$$

where $p(y_k|x)$ is the probability of x being of class y_k . Let the original class, $y_i = C(x)$, be the classifier's output, where i is defined by

$$i = \arg \max_{k \in \{1, \dots, D\}} p(y_k|x). \quad (2)$$

When the classification is inaccurate, the original class differs from the *true class* of the image.

Let \hat{x} be the adversarial example generated from x , such that the *adversarial class*, $y_j = C(\hat{x})$, differs from the *original class*, i.e. $C(\hat{x}) \neq C(x)$. Targeted attacks choose a specific adversarial class [6, 8–13], whereas non-targeted attacks only aim to mislead the classifier [12–15]. Adversarial attacks may also specify that the probability of the adversarial class, $p(y_j|\hat{x})$, should exceed a pre-defined value, σ [12].

To investigate the predictability of mapping between the predicted classes, we visualise the mapping as a weighted bipartite graph, where the nodes are class labels (the same class labels aligned horizontally) and the edges are weighed by the mapping frequency between the classes. The weight of an edge determines its thickness (and opacity): a thicker (and darker) edge indicates a more frequent mapping between the classes. Fig. 1 shows two examples. Fig. 1(a) visualises the class mapping from the true class to the original class of the MNIST training dataset predicted by LeNet classifier [16]. The training dataset contains 60,000 images, distributed unevenly among the true classes¹. LeNet has a classification accuracy of

We thank the Alan Turing Institute (EP/N510129/1), which is funded by the U.K. Engineering and Physical Sciences Research Council, for its support through the project PRIMULA.

*Contact author: chauyi.li@qmul.ac.uk

¹There are between 5,421 and 6,742 instances in each true class.

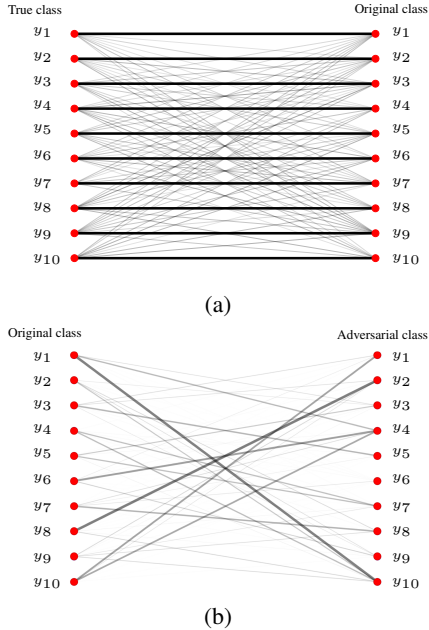


Fig. 1. Mapping between the source class (left nodes) and destination class (right nodes). The thickness (and opacity) of an edge is proportional to the mapping frequency between the two classes. (a) Mapping from the true class to the original class predicted by LeNet classifier on the MNIST [16] training dataset. The classifier has an accuracy of 97.35% on the original images, therefore the horizontal edges dominate. (b) Mapping from the original class to the adversarial class induced by the non-targeted attack N-FGSM [12]. Note that the mapping is not uniform.

97.35% on the original images, resulting in the dominating thick horizontal edges. The thin non-horizontal edges identify the 2.65% inaccurate classifications. Fig. 1(b) visualises the class mapping for the adversarial examples generated by a non-targeted FGSM attack (N-FGSM) [12] for the same classifier and dataset. Note that certain class pairs have thicker edges that indicate a preferential mapping. For example, most images with adversarial class label y_{10} originate from class y_1 . The existence of such preferential mapping indicates the possibility of reversing the adversarial attack and hence retrieving the original class.

3. REVERSIBILITY

We aim to quantify the reversibility of an adversarial attack, which measures the extent to which the original predictions can be retrieved from the adversarial class. To this end, we propose an approach that performs Prediction Reversal from an Adversarial Class (PRAC) by determining the probability that the adversarial class is from a certain original class. PRAC requires the classifier, $C(\cdot)$; a set \mathcal{S} of original images x with original predicted classes covering the D possible classes; and the adversarial classes $y_j = C(\hat{x})$ of the corresponding adversarial examples \hat{x} for all $x \in \mathcal{S}$.

PRAC encodes the probability of the adversarial class $y_j = C(\hat{x})$ being from any of the D original classes in a vector

$$\mathbf{p}_j = (p_j^1, p_j^2, \dots, p_j^D), \quad (3)$$

where p_j^k is the probability that the original images are predicted

Table 1. Reversibility of N-FGSM [12] attacking LeNet on the MNIST dataset [16]. The high original classification accuracy means only a few adversarial examples would select the true class of an image (top-1 accuracy of 1.40%). We report the retrieval accuracy of the top-1 retrieved class matching the original class and the true class using PRAC.

	Classification	Retrieved class	
	accuracy	original	true
Original	97.35		
N-FGSM [12]	1.40	40.15	39.80

to be of the original class y_k . Each p_j^k is defined as the average of $p(y_k|x)$ for all $x \in \mathcal{S}$. This probability can be computed using all but the last layer of $C(\cdot)$, with a prior expectation that the image has an equal probability of being of any one of the D original classes, i.e. $1/D$, as

$$p_j^k = \frac{1}{1 + \sum_{i=1}^D n_{ij}} \left(\frac{1}{D} + \sum_{\substack{x \in \mathcal{S} \\ y_j = C(\hat{x})}} p(y_k|x) \right), \quad (4)$$

where n_{ij} is the number of images with original class $y_i = C(x)$ and adversarial class $y_j = C(\hat{x})$. When none of the images in \mathcal{S} has an adversarial class y_j (hence $n_{ij} = 0$), the probability p_j^k is $1/D$.

When a new adversarial example \hat{x} generated by the same attack is classified as adversarial class $y_j = C(\hat{x})$, PRAC reverses the prediction using \mathbf{p}_j . Specifically, PRAC obtains the top-1 retrieved class as the class y_r with the highest probability in \mathbf{p}_j , where

$$r = \arg \max_{k \in \{1, \dots, D\}} p_j^k. \quad (5)$$

We quantify reversibility as the *retrieval accuracy* of the retrieved class matching the original class or the true class. In particular, the top- k retrieval accuracy, T_k , can be computed from the total number of instances of the corresponding original or true class being in the top- k retrieved classes, R_k , as

$$T_k = \frac{R_k}{N}, \quad (6)$$

where N is the total number of adversarial examples generated by the attack and not in the set \mathcal{S} . A T_5 retrieval accuracy of 50% of matching the original class means that the original class is one of the top-5 retrieved classes in half of the instances.

Tab. 1 shows the reversibility of N-FGSM attacking LeNet for the 10 MNIST classes. The probability vectors \mathbf{p}_j are constructed using the MNIST training set (see mapping in Fig. 1(b)), whereas the retrieval of the class is performed on the MNIST testing set which has 10,000 images. The probability of randomly selecting one class other than the adversarial class and matching the original class is $1/9=11.11\%$, whereas the reversibility of N-FGSM is 40.15%. The original high top-1 classification accuracy of the classifier (97.35%) results in the low top-1 classification accuracy of the adversarial examples generated by N-FGSM. In fact, the adversarial classes of 9,860 of the 10,000 examples (98.60%) are different from their true classes. However, the top-1 class retrieved by PRAC matches the true class for 39.80% of the images (3,980 images), which means that the true class of 40.40% (3,980 divided by 9,860) of the adversarial examples, that concealed the true class, can be retrieved.

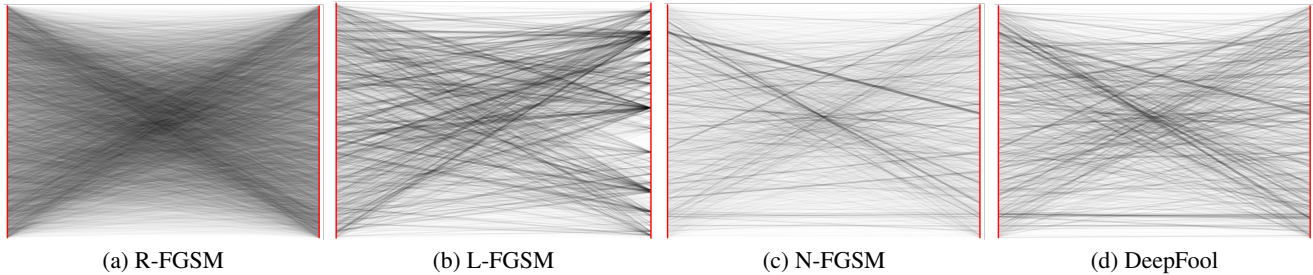


Fig. 2. Class mapping for R-FGSM [11], L-FGSM [12], N-FGSM [12] and DeepFool [14] attacking ResNet-50 classifier [1] on the Places365-Standard dataset [17]. For each sub-image, the set of original classes is on the left, whereas the set of adversarial classes is on the right.

Table 2. Classification accuracy (in percentage) on the original images of the Places-365 Standard validation dataset [17].

DNN	top-1	top-5
AlexNet [2]	46.76	77.66
ResNet-18 [1]	52.67	83.28
ResNet-50 [1]	54.25	84.98

4. RESULTS

4.1. Set-up

We analyse the reversibility of four widely used adversarial attacks: two targeted attacks, namely least-likely FGSM (L-FGSM) [12] and targeted random FGSM (R-FGSM) [11]; and two non-targeted attacks, namely non-targeted FGSM (N-FGSM) [12] and DeepFool [14]. FGSM attacks generate adversarial examples that maximise the cost, computed by the loss function used in training, of remaining in the original class (non-targeted) or that minimise the cost of predicting the targeted class (targeted). L-FGSM selects the least likely class from the original prediction as the target adversarial class, whereas R-FGSM performs the selection of the adversarial class with equal likelihood from all of the classes except the original class. DeepFool iteratively adds perturbations that orthogonally project the image to the nearest linearised class boundary (measured by the Euclidean distance), and eventually crossing the class boundary to induce misclassification. We re-implemented the FGSMs attacks and used the publicly available implementation of DeepFool.

We use as classifiers AlexNet [2], ResNet-18 [1] and ResNet-50 [1] that are trained on the $D=365$ scene classes of the training set of the Places365-Standard dataset [17]. Tab. 2 shows the original classification accuracy of the three classifiers on the validation set: AlexNet has the lowest accuracy and ResNet-50 is the most accurate classifier. Adversarial examples are crafted to change the original prediction of the classifier, thus more accurate classifiers label a larger number of adversarial images with a class that differs from the true class. We randomly split the validation set [17] into two sets of equal size, one for constructing the probability vectors (Eq. 4) and one for quantifying the reversibility of the attack (Eq. 5). Each set has 18,250 images, evenly distributed among the 365 true classes.

Fig. 2 visualises the mapping between original and adversarial classes for the attacks. R-FGSM is a reference of desirable behaviour as the target class is chosen with equal likelihood among all the possible classes. The strong preferential pattern of the targeted attack L-FGSM is caused by the target class selection procedure. The non-targeted attacks, N-FGSM and DeepFool, have similar patterns, due

Table 3. Percentage of non-targeted adversarial classes matching the k^{th} most likely class in the original prediction on the Places-365 Standard dataset [17].

Attack	DNN	Any in 2 nd - 5 th	k^{th} most likely class			
			2 nd	3 rd	4 th	5 th
N-FGSM [12]	AlexNet	58.24	29.90	13.82	8.54	5.98
	ResNet-18	70.38	37.85	16.68	9.35	6.50
	ResNet-50	73.87	41.10	17.02	9.61	6.14
DeepFool [14]	AlexNet	97.14	73.40	13.83	4.68	2.77
	ResNet-18	94.74	67.11	17.11	5.26	5.26
	ResNet-50	92.10	65.79	18.42	5.26	2.63

to the fact that the most probable adversarial classes of an original class label are limited to a few classes. To validate this, Tab. 3 shows the percentage of adversarial classes matching any of the 2nd to 5th most likely classes in the original prediction. The adversarial class by a non-targeted attack often is the second most likely class in the original prediction (41.10% and 65.79% for N-FGSM and DeepFool attacking ResNet-50, respectively), followed by the 3rd and 4th most likely class. Despite the fact that the adversarial class can be any of the $D-1=364$ classes, at least 58.24% adversarial classes of N-FGSM are in fact one of the 2nd to 5th most likely classes in the original prediction. The same observation can be made for DeepFool, with at least 92.10% of the instances matching any of the top 2 to 5 classes.

4.2. Discussion

We discuss the applicability of PRAC and analyse the reversibility of the attacks by reporting the accuracy of the top-1 and top-5 retrieved classes matching the original class and the true class.

We compare PRAC with a baseline frequency counting procedure that retrieves the top- k classes as the k original classes that are most frequently mapped to the adversarial class. Tab. 4 compares the top-5 accuracy of PRAC and the baseline. We do not report the top-1 accuracy as there is little difference in the results. The baseline retrieved 11.90% and 25.32% true classes for L-FGSM and N-FGSM attacking ResNet-50, respectively, whereas PRAC retrieved 15.42% and 32.82%. Note that the baseline gives equal importance to all the original classes, regardless of whether they were accurately classified (i.e. matching the true class), whereas PRAC considers the predicted probabilities by the classifier (Eq. 5), which are often low when the classification is inaccurate. Therefore, PRAC gives more importance to the correctly classified instances and increases the probability of matching the true class.

Table 4. Comparison between a frequency counting baseline and PRAC in terms of top-5 accuracy of the retrieved classes matching the original class and the true class.

Attack	DNN	Original class		True class	
		baseline	PRAC	baseline	PRAC
L-FGSM [12]	AlexNet	17.92	17.92	11.36	15.38
	ResNet-18	17.92	18.20	11.90	15.62
	ResNet-50	17.92	18.22	11.90	15.42
N-FGSM [12]	AlexNet	37.65	37.34	25.12	34.43
	ResNet-18	37.65	37.57	25.13	33.88
	ResNet-50	37.65	37.70	25.32	32.82

Table 5. Classification accuracy on adversarial examples. Reversibility is quantified as the top-1 and top-5 retrieval accuracy, T_1 and T_5 , of classes retrieved with PRAC matching the original class or the true class. All reported values are in percentage.

Attack	DNN	Classifier accuracy		Retrieved class			
		top-1	top-5	original		true	
				T_1	T_5	T_1	T_5
R-FGSM [11]	AlexNet	0.17	8.28	0.15	1.47	0.27	1.44
	ResNet-18	0.11	6.88	0.27	1.44	0.29	1.53
	ResNet-50	0.10	9.30	0.31	1.37	0.33	1.34
L-FGSM [12]	AlexNet	0.03	0.61	5.99	17.92	5.00	15.38
	ResNet-18	0.00	0.41	6.13	18.20	5.15	15.62
	ResNet-50	0.01	0.70	6.04	18.22	5.07	15.42
N-FGSM [12]	AlexNet	14.25	52.60	15.80	37.34	12.41	34.43
	ResNet-18	14.52	56.05	15.84	37.57	12.26	33.88
	ResNet-50	16.72	64.06	16.30	37.70	12.52	32.82
DeepFool [14]	AlexNet	33.41	74.61	15.48	38.12	10.34	30.63
	ResNet-18	36.90	79.95	17.52	44.02	12.15	35.63
	ResNet-50	42.54	82.59	18.68	44.48	13.15	36.48

Tab. 5 shows the retrieval accuracy on the four adversarial attacks (Eq. 5). The reversibility of an attack does not change significantly across the three classifiers. This is expected as reversibility is a property of the attack, not the classifier. For non-targeted attacks, PRAC retrieves for N-FGSM on AlexNet the original class from the top-1 and top-5 15.80% and 37.34% of the times, respectively. DeepFool is the most reversible attack as PRAC can retrieve the original class from the top-5 classifications with an accuracy of 38.12% for AlexNet and at least 44.48% for ResNet-18 and ResNet-50. As for targeted attacks, R-FGSM, which randomly selects one out of the 364 classes as the target class, is the least reversible attack with a top-1 retrieval accuracy between 0.10% and 0.17% across classifiers. L-FGSM, which selects the least-likely original class as the target class, has the original class retrieved at least 5.99% of the instances (i.e. the original class is retrieved for at least 1,108 adversarial examples).

To analyse the possibility of the retrieved classes matching the true class, Tab. 5 reports the accuracy of the true class matching the top-1 and the top-5 retrieved classes, and also the accuracy of the classifier on the adversarial examples. DeepFool has the smallest effect on classification accuracy and its adversarial effect is highly reversible. In particular, the retrieved class of DeepFool attacking ResNet-50 matches the true class at 36.48% for top-5, which is equivalent to 42.90% (36.48% divided by 84.98%) of the classifier’s original accuracy (Tab. 2). L-FGSM has the largest impact on

Table 6. Effect on the reversibility of specifying a minimum value σ for the adversarial class probability when using N-FGSM [12] attacking AlexNet [2] on the Places365-Standard dataset [17]. N/A means that the only objective for the attack is to mislead the classifier, not to reach a specific probability for the adversarial class.

σ	Retrieved original class	
	T_1	T_5
N/A	15.80	37.34
.6	10.34	24.48
.7	9.52	23.06
.8	8.77	22.23
.9	8.29	21.59

classification accuracy, which varies between 0.00% and 0.03% for top-1, and between 0.41% and 0.70% for top-5. However, the retrieved class matches the true class with a relatively high accuracy (minimum 5% and 15.38% for top-1 and top-5, respectively). This large discrepancy between the low classification accuracy and top true class retrieval accuracy suggests that, when designing an adversarial attack, more objectives than just a low classification accuracy, should be considered to avoid the attack to be reversed.

We finally investigate the effect of specifying the adversarial class probability on the reversibility of the non-targeted N-FGSM. Tab. 6 shows the reversibility when the adversarial class probability is forced to exceed $\sigma \in \{0.6, 0.7, 0.8, 0.9\}$ for N-FGSM attacking AlexNet. We note that the average predicted probability of the adversarial classes without specifying the probability (i.e. only aiming to mislead the classifier) is 0.48. The larger σ , the less reversible the attack. We believe that this happens because the preferential mapping that contributes to the high reversibility of non-targeted attacks (Tab. 3) is weakened. In particular, as σ increases and becomes larger than the average probability of 0.48, the attack cannot attain such a high probability with its original preferential class mapping and seeks another class as the adversarial one, resulting in a lower reversibility.

5. CONCLUSION

We discussed the reversibility of adversarial attacks, namely the possibility of retrieving the original class of an adversarial image and hence reversing the attack. We demonstrated how to perform Prediction Reversal from the Adversarial Class (PRAC) by exploiting the mapping between original and adversarial classes. PRAC supports the design of more effective adversarial attacks as well as the design of new defences. We quantified the reversibility as the accuracy of the original class being among the top- k retrieved classes, and also investigated the possibility of retrieving the true class. Furthermore, we analysed the factors affecting the reversibility of an attack. Notably, the high reversibility of non-targeted attacks is caused by the high probability of the adversarial class being of one of the top most likely classes. Moreover, specifying a higher probability of the adversarial class reduces the reversibility of non-targeted attacks.

6. REFERENCES

- [1] K. He, S. Zhang, X. Ren, and J. Sun, "Deep residual learning for image recognition," in *Proceedings of the IEEE Conference on Computer Vision and Pattern Recognition*, June 2016, pp. 770–778.
- [2] A. Krizhevsky, I. Sutskever, and G. Hinton, "ImageNet classification with deep convolutional neural networks," in *Proceedings of the Advances in Neural Information Processing Systems*, January 2012, vol. 25, pp. 1097–1105.
- [3] C. Szegedy, W. Zaremba, I. Sutskever, J. Bruna, D. Erhan, I. Goodfellow, and R. Fergus, "Intriguing properties of neural networks," in *International Conference on Learning Representations*, Banff, Canada, April 2014.
- [4] I. Goodfellow, J. Shlens, and C. Szegedy, "Explaining and harnessing adversarial examples," in *International Conference on Learning Representations*, San Diego, USA, May 2015.
- [5] F. Tramèr, N. Papernot, I. Goodfellow, D. Boneh, and P. McDaniel, "The space of transferable adversarial examples," *arXiv preprint arXiv:1704.03453*, April 2017.
- [6] C.Y. Li, A.S. Shamsabadi, R. Sanchez-Matilla, R. Mazzon, and A. Cavallaro, "Scene privacy protection," in *Proceedings of the IEEE International Conference on Acoustics, Speech and Signal Processing*, May 2019, pp. 2502–2506.
- [7] M. Abbasi and C. Gagné, "Robustness to adversarial examples through an ensemble of specialists," *arXiv preprint arXiv:1702.06856*, Mar. 2017.
- [8] N. Papernot, P. McDaniel, S. Jha, M. Fredrikson, Z. Celik, and A. Swami, "The limitations of deep learning in adversarial settings," in *IEEE European Symposium on Security and Privacy*, Saarbrücken, Germany, March 2016.
- [9] N. Carlini and D. Wagner, "Towards evaluating the robustness of neural networks," in *IEEE symposium on Security and Privacy*, San Jose, California, USA, May 2017.
- [10] F. Tramèr, A. Kurakin, N. Papernot, I. Goodfellow, D. Boneh, and P. McDaniel, "Ensemble adversarial training: Attacks and defenses," in *International Conference on Learning Representations*, Vancouver, Canada, April 2018.
- [11] A. Kurakin, I. Goodfellow, and S. Bengio, "Adversarial machine learning at scale," in *International Conference on Learning Representations*, Toulon, France, April 2017.
- [12] A. Kurakin, I. Goodfellow, and S. Bengio, "Adversarial examples in the physical world," in *International Conference on Learning Representations Workshop Track*, Toulon, France, April 2017.
- [13] C. Xie, Z. Zhang, J. Wang, Y. Zhou, Z. Ren, and A. Yuille, "Improving transferability of adversarial examples with input diversity," in *Proceedings of the IEEE Conference on Computer Vision and Pattern Recognition*, June 2019, pp. 2730–2739.
- [14] S. Moosavi-Dezfooli, A. Fawzi, and P. Frossard, "DeepFool: A simple and accurate method to fool deep neural networks," in *Proceedings of the IEEE Conference on Computer Vision and Pattern Recognition*, June 2016, pp. 2574–2582.
- [15] A. Modas, S. Moosavi-Dezfooli, and P. Frossard, "SparseFool: A few pixels make a big difference," in *Proceedings of the IEEE Conference on Computer Vision and Pattern Recognition*, June 2019, pp. 9079–9088.
- [16] Y. Lecun, L. Bottou, Y. Bengio, and P. Haffner, "Gradient-based learning applied to document recognition," *Proceedings of the IEEE*, vol. 86, no. 11, pp. 2278–2324, November 1998.
- [17] B. Zhou, A. Lapedriza, A. Khosla, A. Oliva, and A. Torralba, "Places: A 10 million image database for scene recognition," *IEEE Transactions on Pattern Analysis and Machine Intelligence*, vol. 40, no. 6, pp. 1452–1464, June 2018.